The Astrophysical Journal Letters, 886:L27 (5pp), 2019 December 1 https://doi.org/10.3847/2041-8213/ab552d

An Improved Distance to NGC 4258 and Its Implications for the Hubble Constant

M. J. Reid[1], D. W. Pesce[1,2], and A. G. Riess[3,4]
[1] Center for Astrophysics | Harvard & Smithsonian, 60 Garden Street, Cambridge, MA 02138, USA
[2] Black Hole Initiative at Harvard University, 20 Garden Street, Cambridge, MA 02138, USA
[3] Department of Physics and Astronomy, Johns Hopkins University, Baltimore, MD, USA
[4] Space Telescope Science Institute, Baltimore, MD, USA
Received 2019 August 14; revised 2019 October 14; accepted 2019 November 6; published 2019 November 22

Abstract

NGC 4258 is a critical galaxy for establishing the extragalactic distance scale and estimating the Hubble constant (H_0). Water masers in the nucleus of the galaxy orbit about its supermassive black hole, and very long baseline interferometric observations of their positions, velocities, and accelerations can be modeled to give a geometric estimate of the angular-diameter distance to the galaxy. We have improved the technique to obtain model parameter values, reducing both statistical and systematic uncertainties compared to previous analyses. We find the distance to NGC 4258 to be 7.576 ± 0.082 (stat.) ± 0.076 (sys.) Mpc. Using this as the sole source of calibration of the Cepheid-SN Ia distance ladder results in $H_0 = 72.0 \pm 1.9$ km s^{-1} Mpc^{-1}, and in concert with geometric distances from Milky Way parallaxes and detached eclipsing binaries in the LMC we find $H_0 = 73.5 \pm 1.4$ km s^{-1} Mpc^{-1}. The improved distance to NGC 4258 also provides a new calibration of the tip of the red giant branch of $M_{F814W} = -4.01 \pm 0.04$ mag, with reduced systematic errors for the determination of H_0 compared to the LMC-based calibration, because it is measured on the same *Hubble Space Telescope* (*HST*) photometric system and through similarly low extinction as SN Ia host halos. The result is $H_0 = 71.1 \pm 1.9$ km s^{-1} Mpc^{-1}, in good agreement with the result from the Cepheid route, and there is no difference in H_0 when using the same calibration from NGC 4258 and the same SN Ia Hubble diagram intercept to start and end both distance ladders.

Unified Astronomy Thesaurus concepts: Observational cosmology (1146); Galaxy distances (590)

1. Introduction

The nucleus of NGC 4258 hosts a H_2O megamaser in a sub-parsec-scale accretion disk surrounding a $4 \times 10^7\,M_\odot$ black hole. Very long baseline interferometric (VLBI) mapping and spectral monitoring of the masers yield estimates of angular and linear accelerations of masing clouds in their Keplerian orbits about the black hole. Combining these accelerations yields a very accurate and purely geometric distance to the galaxy. The distance to NGC 4258 provides an important calibration for the Cepheid period–luminosity (PL) relation and the absolute magnitude of the tip of the red giant branch (TRGB). These calibrations, in turn, provide the basis for some of the most accurate estimates of the Hubble constant (H_0).

Humphreys et al. (2013) analyzed the very extensive data set of observations of the H_2O masers toward NGC 4258 presented by Argon et al. (2007) and Humphreys et al. (2007) and estimated a distance of 7.60 ± 0.17 (stat.) ± 0.15 (sys.) Mpc. The fitted data consisted of positions in two dimensions, Doppler velocities, and line-of-sight accelerations of individual maser features. The statistical (stat.) distance uncertainty was estimated using a likelihood function that depended, in part, on assumed values for "error floors." These error floors were added in quadrature to measurement uncertainty in order to account for unknown limitations in the data, including "astrophysical noise." For example, the $6_{1,6} - 5_{2,3}$ H_2O transition has six hyperfine components, with three dominant components spanning 1.6 km s^{-1}. When calculating a Doppler velocity one generally assumes that the three dominant components contribute equally to the line profile. However, were one of the outer components to dominate the maser amplification, this could shift the assigned line velocity by 0.8 km s^{-1}.

The heterogeneous nature of the data precludes a simple scaling of data uncertainties in order to achieve a post-fit χ^2_ν per degree of freedom of unity. Since there are no strong priors on the values of the error floors, reasonable variations in these values contribute to the estimated systematic (sys.) uncertainty. In order to better address these issues, we have reanalyzed the NGC 4258 data using a Markov Chain Monte Carlo (MCMC) approach, which includes the error floors as adjustable parameters. Owing to the exquisite quality of the data set, these parameters could be solved for using "flat" priors, with only non-negative restrictions on the their values. This approach indicated that the position error floors used by Humphreys et al. (2013) were overly conservative, and that properly accounting for them reduced the statistical uncertainty in distance, while also removing their contribution to systematic uncertainty. In this Letter, we report a revised distance to NGC 4258 and, correspondingly, estimates of H_0 with reduced uncertainty.

2. An Improved Distance Estimate for NGC 4258

Over the past 25 yr, the number of VLBI observations used to map the masers in NGC 4258 and measure their accelerations has dramatically increased. Table 1 summarizes the geometric distance estimates based on modeling the Keplerian orbits of maser features about the galaxy's supermassive black hole. The distance estimates reported in the first three papers listed in the table were based on successively larger data sets and, therefore, are nearly statistically independent. These distance estimates are statistically consistent. The last three papers (i.e., starting with Humphreys et al. 2013) used the same data set, with the latter two papers improving the analysis approach. These papers report only very

Table 1
Estimates of Distance to NGC 4258

Reference	Distance (Mpc)	(Stat., Sys.) (Mpc)	Data	Comment
Miyoshi et al. (1995)	6.4 ± 0.9	(0.9, n.a.)	1 VLBI epoch	...
Herrnstein et al. (1999)	7.2 ± 0.5	(0.3, 0.4)	4 VLBI epochs	...
Humphreys et al. (2013)	7.596 ± 0.228	(0.167,0.155)	18 VLBI epochs	...
Riess et al. (2016)	7.540 ± 0.197	(0.170,0.100)	18 VLBI epochs	Better MCMC convergence
This paper	7.576 ± 0.112	(0.082,0.076)	18 VLBI epochs	Improved analysis (see text)

Note. Distance uncertainties are the quadrature sum of the statistical (Stat.) and systematic (Sys.) errors. The distance modulus from this Letter is 29.397 ± 0.032.

Table 2
Fitted Disk Model

Parameter	This Letter	Humphreys et al. (2013)
Disk Fitting Parameters[a]		
Distance (Mpc)	7.576 ± 0.082	7.596 ± 0.170
black hole mass (10^7 $M_\odot$)	3.98 ± 0.04	4.00 ± 0.09
Galaxy systemic velocity (km s^{-1})	473.3 ± 0.4	474.2 ± 0.5
Dynamical center[b] x-position (mas)	−0.152 ± 0.003	−0.204 ± 0.005
Dynamical center[b] y-position (mas)	0.556 ± 0.004	0.560 ± 0.006
Disk inclination[c] (deg)	87.05 ± 0.09	86.93 ± 0.22
Inclination warp 1st order (deg mas^{-1})	2.59 ± 0.07	2.49 ± 0.11
Inclination warp 2nd order (deg mas^{-2})	0.041 ± 0.018	...
Disk position angle[c] (deg)	88.43 ± 0.04	88.43 ± 0.14
Position angle warp 1st order (deg mas^{-1})	2.21 ± 0.02	2.30 ± 0.06
Position angle warp 2nd order (deg mas^{-2})	−0.13 ± 0.01	−0.24 ± 0.02
Orbital Eccentricity	0.007 ± 0.001	0.006 ± 0.001
Periapsis angle (deg)	318 ± 13	294 ± 64
Periapsis angle warp (deg mas^{-1})	123 ± 7	60 ± 10
Error Floors[d]		
σ_x eastward offset (mas)	0.0016 ± 0.0005	[0.0200]
σ_y northward offset (mas)	0.0041 ± 0.0005	[0.0300]
$\sigma_{v,\mathrm{sys}}$ systemic velocities (km s^{-1})	0.31 ± 0.20	[1.00]
$\sigma_{v,\mathrm{hv}}$ high-vel velocities (km s^{-1})	2.25 ± 0.31	[1.00]
σ_a accelerations (km s^{-1} y^{-1})	0.46 ± 0.04	[0.30]

Notes.
[a] Uncertainties are formal statistical estimates, inflated by their respective $\sqrt{\chi^2_\nu}$.
[b] Positions are measured relative to the maser emission at 510 km s^{-1}. The difference between the x-position values is largely due to the systematic effect of changing the recessional velocity from relativistic in Humphreys et al. (2013) to $(1 + z)$ in this Letter.
[c] Disk inclination and position angle are measured at a radius, r, of 6.1 mas, near the average radius of the masers. The values from Humphreys et al. (2013) have been adjusted from $r = 0$ to $r = 6.1$ mas.
[d] Brackets for the Humphreys et al. (2013) error floor values indicate that these were assumed and not solved for.

small changes in the estimated distance, but with successive improvements in the uncertainty.

The dynamics of an H_2O maser cloud in an accretion disk surrounding a supermassive black hole can be characterized by four measurements: the eastward and northward offsets from a fiducial position, (x, y); its heliocentric Doppler velocity, V; and its line-of-sight acceleration, A. The relative weightings of these heterogeneous data can affect model fitted parameters. Whereas previously one had the freedom to adjust the individual error floors for these data components, we now remove this freedom and incorporate the error floors as parameters that are adjusted automatically with each MCMC trial. This removes potential bias and "lets the data speak." Note that in order to allow for adjustable data weights, one must include the $\frac{1}{\sigma}$ pre-factor in the full Gaussian formula, $\frac{1}{\sqrt{2\pi}}\frac{1}{\sigma}e^{-\Delta^2/2\sigma^2}$, when evaluating data uncertainties for the likelihood calculation (e.g., Roe 2015). We have conducted tests on mock data sets of megamaser disks, which were generated with different levels of Gaussian random noise, and we were able to recover those noise levels. Thus, we are confident that this procedure works well.

The position error floors previously adopted by Humphreys et al. (2013) were $(\sigma_x, \sigma_y) = (\pm 0.010, \pm 0.020)$ mas. These were based on very conservative estimates of the effects of potential interferometric delay errors. Allowing the error floors to be model parameters revealed that the uncertainty of the relative positions measured by VLBI actually approach $(\pm 0.002, \pm 0.004)$ mas accuracy for high signal-to-noise maser spots across the small field of view of the accretion disk (±7 mas). Re-fitting the data of Humphreys et al., we obtain the parameters listed in Table 2. Specifically, we find $D = 7.576 \pm 0.075$ (stat.) Mpc, where the formal statistical uncertainty is

now a factor of two smaller than before. The reduced χ^2_ν for this fit is 1.2 (for 483 degrees of freedom), which is an improvement over the reduced χ^2_ν of 1.4 in Humphreys et al. (2013), and we conservatively inflate the statistical component of distance uncertainty by $\sqrt{1.2}$ leading to ± 0.082 Mpc.

The MCMC fitting code of Humphreys et al. (2013) employs the Metropolis–Hastings algorithm. Modifications to that program were (1) to allow the error floors to be adjustable parameters, (2) to replace handling of the recessional velocity from a relativistic velocity to the standard $(1 + z)$ formalism, and (3) to define the warping parameters relative to the average maser radius (6.1 mas) instead of at the origin. As an end-to-end check on this code, one of us (DP) has written an independent fitting program, implementing a Hamiltonian MCMC approach, and we find essentially identical results from both programs The two-dimensional marginalized probability densities for selected parameters are shown in Figure 1.

Further gains in distance accuracy come from reducing systematic sources of error. Humphreys et al. (2013), in their Table 4, listed the contributions of a number of systematics to the distance uncertainty. By solving for error floor parameters, their uncertainties are now incorporated into the marginalized distance estimate, and therefore we remove their contributions from the systematic error budget. In addition, as done in Riess et al. (2016), we now calculate two orders of magnitude more MCMC trials than in Humphreys et al. (2013), making the fitted parameter values largely insensitive to initial conditions. Finally, since we allow for eccentric orbits for the masing clouds, as well as second-order warping of the disk, the marginalized distance estimate now includes these uncertainties. The only remaining systematic error term in Table 4 of Humphreys et al. that we have not included in our distance uncertainty is their estimate of the effects of unmodeled spiral structure of ± 0.076 Mpc. Thus, we have now reduced the estimated systematic uncertainty by nearly a factor of two.

Our best estimate of the distance to NGC 4258 is 7.576 ± 0.082 (stat.) $\pm$ 0.076 (sys.) Mpc.

3. Estimate of H_0

NGC 4258 has played a central role in the determination of the Hubble constant, because its geometric distance has been established to useful and increasingly high precision since Herrnstein et al. (1999). The galaxy is near enough to calibrate Cepheid variables (Maoz et al. 1999; Macri et al. 2006; Hoffman 2013), TRGB (Macri et al. 2006; Mager et al. 2008; Jang & Lee 2017), and Mira variables (Huang et al. 2018) using the *Hubble Space Telescope* (*HST*). These stars in turn are used to calibrate the luminosities of SNe Ia, which measure the Hubble flow and the Hubble constant.

In order to determine the Hubble constant using the improved distance to NGC 4258 presented here, we use the Cepheid and SN Ia data and formalism presented in Riess et al. (2016) and revised geometric distances provided in Riess et al. (2019). The distance to NGC 4258 has increased modestly from that in Riess et al. (2016) by 0.5%, well within the total $\pm 2.6\%$ error there, or even the $\pm 1.5\%$ total error here, resulting in a small change in H_0 measured using NGC 4258 as the sole, geometric calibrator of Cepheid luminosities. However, there is a larger impact on H_0 measured in conjunction with the other geometric calibrators: Milky Way parallaxes and detached eclipsing binaries (DEBs) in the LMC (Pietrzyński et al. 2019). The reason is that the weight of NGC 4258 in the joint solution has increased substantially due to its 40% smaller distance error, and its preferred value for H_0 is 2.7% lower than for the other methods. Including uncertainties in the PL relationships and photometric zero-points given in Table 6 of Riess et al. (2019), the net uncertainties in the use of each anchor for the Cepheid distance ladder are now 2.1%, 1.7% and 1.5% for NGC 4258, Milky Way parallaxes, and the LMC DEBs, respectively. The values of H_0 and their uncertainties (including systematics) are given in Table 3. Combining estimates from all three anchors yields a best value for H_0 of 73.5 ± 1.4 km s^{-1} Mpc^{-1}, with the revised distance to NGC 4258 reducing H_0 by this combination by 0.7%. The total uncertainty is little changed because the error is already dominated by the mean of the 19 SN Ia calibrators from Riess et al. (2016) (1.2%), with little impact from the reduction of the error due to the geometric calibration of Cepheids which decreases here from 0.8% to 0.7%. The difference between this late universe measurement of H_0 and the prediction from Planck and ΛCDM (Planck 2018) of 67.4 ± 0.5 km s^{-1} Mpc^{-1} remains high at 4.2σ.

We can also use the revised distance to NGC 4258 to derive a new calibration of the TRGB on the *HST* ACS photometric system, which is used to observe the TRGB in the halos of SN Ia hosts. There are two sets of *HST* observations with the ACS in *F*814*W* that have yielded a strong detection of the TRGB in NGC 4258: GO 9477 (PI: Madore, 2.6 ks in *F*814*W*) and GO 9810 (PI: Greenhill, 8.8 ks in *F*814*W*). The GO 9477 observation is of a halo field and has been analyzed by Mager et al. (2008), Madore et al. (2009), and Jang & Lee (2017), with differing definitions of the TRGB magnitude system (e.g., color transformed in Madore et al. 2009). The recent thorough analysis by Jang & Lee (2017) find $\mathrm{F814W}_0 = 25.36 \pm 0.03$ mag, where a foreground extinction of $A_{F814W} = 0.025 \pm 0.003$ mag was assumed.

One expects that there will only be a small amount of extinction of the TRGB in the halos of galaxies. A statistical value of $A_I \sim 0.01$ mag is indicated from an analysis by Ménard et al. (2010) based on the reddening of background quasars by foreground halos at radii from the host center of 10–20 kpc (Ménard et al. 2010). Most importantly for the determination of H_0 is to use a *consistent* approach to estimate the TRGB extinction, both where the TRGB is calibrated and where that calibration is applied, to better reduce systematic errors through their cancellation. In this manner the determination of H_0 is relatively independent of whether or not halos have a measurable amount of extinction, and for this reason we default to the convention of assuming no halo extinction.

Macri et al. (2006) measured the TRGB in the "Outer field" of NGC 4258 using data from GO 9810. This field is primarily from the halo of NGC 4258 and is at a similar separation from the nucleus, $r \sim 20$ kpc, as other TRGB measurements used in Freedman et al. (2019) and where internal extinction is by convention assumed to be negligible. The observation is very deep, reaching $I \sim 27$ and $V \sim 28$, significantly deeper than the TRGB magnitude and sufficient to reject all stars in the *I*-band luminosity function with $V - I \leqslant 1$ mag. The apparent TRGB is $I = 25.42 \pm 0.02$ mag or transformed using Equation (2) in Macri et al. (2006) for the TRGB color of $V - I = 1.6$ mag and the small color term back to the *HST* system of $F814W = 25.398 \pm 0.02$ mag. This detection is somewhat stronger in this data than from GO program 9477, likely due to its greater depth (2.6 ks versus 8.8 ks in *F*814*W*) and is reflected in its smaller error (both generated by a bootstrap

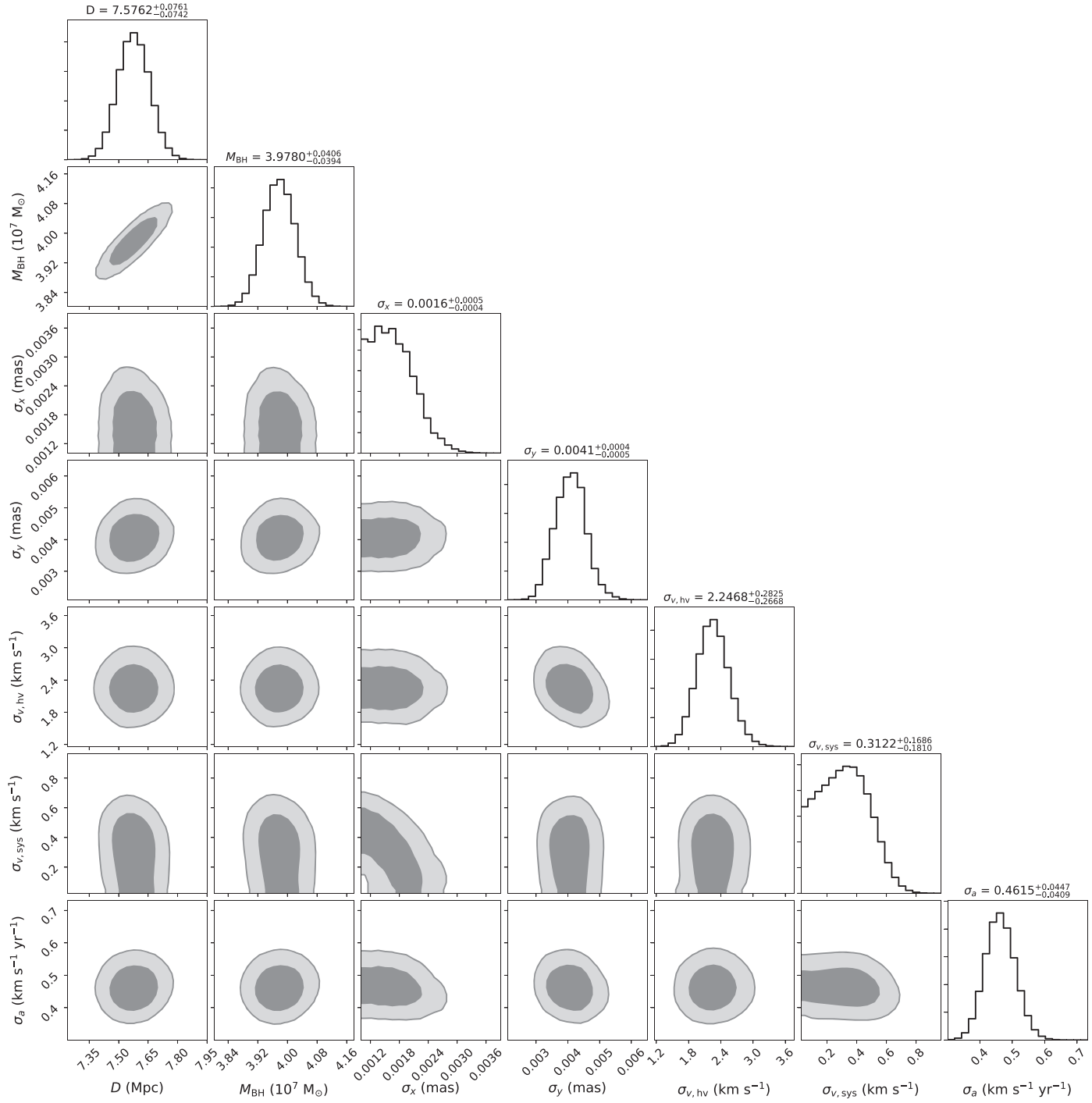

Figure 1. Marginalized probability densities for selected parameters: distance (D), black hole mass (M_{bh}), and error floors for the eastward (σ_x) and northward (σ_y) positions, the high ($\sigma_{v,hv}$) and systemic ($\sigma_{v,sys}$) velocities, and the accelerations (σ_a).

test). The outer chip of this field (no disk, only halo) gives the same estimated peak to $<0.5\sigma$ (L. Macri 2004 private communication). Correcting this by the same amount as the Jang & Lee (2017) result for Milky Way extinction yields very good agreement (1σ) with the result from Jang & Lee. We take the average of the two and conservatively adopt the larger error (as these errors may be correlated via edge detection methods and point-spread function fitting packages used) resulting in $F814W = 25.385 \pm 0.030$ mag. Using the distance to NGC 4258 presented here, which translates to $\mu_{N4258} = 29.397 \pm 0.032$ mag, yields $M_{F814W} = -4.01 \pm 0.04$ mag for the TRGB.

Although the distance uncertainty is a bit larger for NGC 4258 than for the LMC, systematic errors in the TRGB measurement of H_0 calibrated with NGC 4258 are smaller because (i) this calibration is on the same *HST* photometric system (zero-points, instruments, bandpasses) as TRGB measured in SN Ia hosts, (ii) the extinction is either negligible as assumed in SN Ia host halos or, even if $\sim$0.01 mag, it

Table 3
Estimates of H_0 Including Systematics Using Cepheids

Anchor(s)	H_0 value (km s^{-1} Mpc^{-1})	Difference from (Planck+ΛCDM)[a]
NGC 4258	72.0 ± 1.9	2.4σ
Two anchors		
LMC + NGC 4258	72.7 ± 1.5	3.4σ
LMC + MW	74.5 ± 1.5	4.5σ
NGC 4258 + MW	73.1 ± 1.5	3.6σ
Three anchors (best)		
NGC 4258 + MW + LMC	73.5 ± 1.4	4.2σ

Note.
[a] $H_0 = 67.4 \pm 0.5$ km s^{-1} Mpc^{-1} (Planck 2018).

Table 4
Estimates of H_0 Including Systematics Using TRGB

Anchor(s)	H_0 Value[a] (km s^{-1} Mpc^{-1})	Difference from (Planck+ΛCDM)[b]
NGC 4258[c]	70.3 ± 1.9	1.5σ
NGC 4258[d]	71.5 ± 1.9	2.2σ
NGC 4258[e]	71.1 ± 1.9	1.9σ

Notes.
[a] TRGB and Cepheids use different SN Ia intercepts as discussed in the text.
[b] $H_0 = 67.4 \pm 0.5$ km s^{-1} Mpc^{-1} (Planck 2018).
[c] Based on a foreground extinction corrected TRGB peak of $F814W = 25.36 \pm 0.03$ mag from the GO 9477 (PI: Madore) data by Jang & Lee (2017).
[d] Based on a foreground extinction corrected TRGB peak of $F814W = 25.398 \pm 0.033$ mag from the GO 9810 (PI: Greenhill) data Macri et al. (2006).
[e] Using Jang & Lee (2017) and Macri et al. (2006) variance-weighted average of $F814W = 25.385 \pm 0.022$ mag.

becomes negligible after a consistent treatment through its cancellation along the distance ladder, and (iii) the metallicity in the halos of large galaxies is likely to be more similar to each other (i.e., metal-poor) than to the LMC. Indeed, the present shortcomings of the LMC TRGB calibration are that it has been measured only with ground-based systems (Jang & Lee 2017), which have low angular resolution that results in blending of ∼0.02 mag (Yuan et al. 2019), and extinction of the TRGB toward the LMC is a substantial $A_I \geqslant 0.1$ mag and difficult to estimate, with differences in recent estimates of $A_I \approx 0.06 \pm 0.02$ mag (Jang & Lee 2017; Freedman et al. 2019; Yuan et al. 2019).

Replacing the calibration of the TRGB of $F814W = -4.01 \pm 0.04$ mag derived from the improved distance to NGC 4258 on the *HST* (i.e., native) photometric system with the value used by Freedman et al. (2019) of $F814W = -4.05 \pm 0.04$ mag and using their SN Ia TRGB sample yields $H_0 = 71.1 \pm 1.9$ km s^{-1} Mpc^{-1}. This value is in excellent agreement with that derived using Cepheids calibrated by the distance to NGC 4258 of $H_0 = 72.0 \pm 1.9$ km s^{-1} Mpc^{-1} (see Table 3). We also provide the individual values of H_0 using the two previously described TRGB measurements in NGC 4258 in Table 4.

An additional consideration for comparing these two distance ladders is that each used a different sample of SN Ia to measure the Hubble flow. Riess et al. (2016) used a homogeneously calibrated "Supercal" compilation of surveys (Scolnic et al. 2015), and Freedman et al. (2019) used a sample from the Carnegie Supernova Program (CSP; Burns et al. 2018). Because most of the data for the SNe in TRGB or Cepheid hosts is also derived from other non-CSP surveys, there is a preference for the use of a homogeneously calibrated compilation at both ends of the ladder to reduce systematic errors between samples. The CSP sample used with the TRGB produces an intercept that is ∼1% lower (in H_0) than the intercept from the compilation set (Burns et al. 2018; Kenworthy et al. 2019) used with Cepheids, and this 1% difference is the same as the remaining difference in H_0 from the TRGB and Cepheid route. Thus, we find using the geometric calibration from NGC 4258 and the same Hubble diagram intercept for both the TRGB and Cepheid distance ladders brings them into agreement.

Facilities: VLBA, *HST*.

ORCID iDs

M. J. Reid https://orcid.org/0000-0001-7223-754X
D. W. Pesce https://orcid.org/0000-0002-5278-9221

References

Argon, A. L., Greenhill, L. J., Reid, M. J., Moran, J. M., & Humphreys, E. M. L. 2007, ApJ, 659, 1040
Burns, C. R., Parent, E., Phillips, M. M., et al. 2018, ApJ, 869, 56
Freedman, W. L., Madore, B. F., Hatt, D., et al. 2019, ApJ, 882, 34
Herrnstein, J. R., Moran, J. M., Greenhill, L. J., et al. 1999, Natur, 400, 539
Hoffman, S. L. 2013, PhD Thesis, Texas A&M Univ.
Huang, C. D., Riess, A. G., Hoffmann, S. L., et al. 2018, ApJ, 857, 67
Humphreys, E. M. L., Reid, M. J., Greenhill, L. J., Moran, J. M., & Argon, A. L. 2007, ApJ, 672, 800
Humphreys, E. M. L., Reid, M. J., Moran, J. M., Greenhill, L. J., & Argon, A. L. 2013, ApJ, 775, 13
Jang, I. S., & Lee, M. G. 2017, ApJ, 836, 74
Kenworthy, W. D., Scolnic, D., & Riess, A. 2019, ApJ, 875, 145
Macri, L. M., Stanek, K. Z., Bersier, D., Greenhill, L. J., & Reid, M. J. 2006, ApJ, 652, 1133
Madore, B. F., Mager, V. A., & Freedman, W. L. 2009, ApJ, 690, 389
Mager, V. A., Madore, B. F., & Freedman, W. L. 2008, ApJ, 689, 721
Maoz, E., Newman, J. A., Ferrarese, L., et al. 1999, Natur, 401, 351
Ménard, B., Kilbinger, M., & Scranton, R. 2010, MNRAS, 406, 1815
Ménard, B., Scranton, R., Fukugita, M., & Richards, G. 2010, MNRAS, 405, 1025
Miyoshi, M., Moran, J., Herrnstein, J., et al. 1995, Natur, 373, 127
Pietrzyński, G., Graczyk, D., Gallenne, A., et al. 2019, Natur, 567, 200
Planck, 2018, Results VI Cosmological Parameters, arXiv:1807.06209
Riess, A. G., Casertano, S., Yuan, W., Macri, L. M., & Scolnic, D. 2019, ApJ, 876, 85
Riess, A. G., Macri, L. M., Hoffmann, S. L., et al. 2016, ApJ, 826, 56
Roe, B. 2015, arXiv:1906:09077
Scolnic, D., Casertano, S., Riess, A., et al. 2015, ApJ, 815, 117
Yuan, W., Riess, A. G., Macri, L. M., et al. 2019, arXiv:1908.00993